Article

Managing Local Order in Conjugated Polymer Blends via Polarity Contrast

Matthew J Dyson, Eirini Lariou, Jaime Martin, Ruipeng Li, Harikrishna Erothu, Guillaume Wantz, Paul D Topham, Olivier J. Dautel, Sophia C. Hayes, Paul N. Stavrinou, and Natalie Stingelin

Just Accepted

1
2
3
4
5
6
7
8
9
10
11
12
13
14
15
16
17
18
19
20
21
22
23
24
25
26
27
28
29
30
31
32
33
34
35
36
37
38
39
40
41
42
43
44
45
46
47
48
49
50
51
52
53
54
55
56
57
58
59
60

Managing Local Order in Conjugated Polymer Blends via Polarity Contrast

Matthew J. Dyson*,[†,‡] Eirini Lariou,[§] Jaime Martin,[‖,¶] Ruipeng Li,[#] Harikrishna Erothu,[□, Δ] Guillaume Wantz,[◊] Paul D. Topham,[□] Olivier J. Dautel,[♦] Sophia C. Hayes*,[§] Paul N. Stavrinou,[∇] Natalie Stingelin*,[□,■,○]

† Molecular Materials and Nanosystems, Institute for Complex Molecular Systems, Eindhoven University of Technology, P.O. Box 513, 5600 MB Eindhoven, Netherlands

‡ Department of Physics and Centre for Plastic Electronics, Imperial College London, Exhibition Rd, London, SW7 2AZ, UK

§Department of Chemistry, University of Cyprus, P.O. Box 20537, 1678, Nicosia, Cyprus

‖ POLYMAT, University of the Basque Country UPV/EHU, Avenida de Tolosa 72, 20018 Donostia-San Sebastián, Spain

¶ Ikerbasque, Basque Foundation for Science, 48013 Bilbao, Spain

National Synchrotron Light Source II, Brookhaven National Lab, Upton, New York, USA

▨ Aston Institute of Materials Research, Aston University, Birmingham, B4 7ET

Δ Centre for Advanced Energy Studies (CAES), Koneru Lakshmaiah Education Foundation, Green Fields, Vaddeswaram, Guntur District, Andhra Pradesh-522 502, India

◊ Université de Bordeaux, IMS, CNRS, UMR-5218, Bordeaux INP, ENSCBP, 33405 Talence, France

♦ Institut Charles Gerhardt de Montpellier, Laboratoire AM2N, UMR-5253, Université de Montpellier, ENSCM, CNRS, 8 rue de l'École Normale, 34296 Montpellier cedex 5, France

∇ Department of Engineering Science, University of Oxford, Parks Rd, OX1 3PJ, UK

□ School of Materials Science & Engineering and School of Chemical & Biomolecular Engineering, Georgia Institute of Technology, Ferst Drive, Atlanta, Georgia 30332, USA

■ Department of Materials and Centre for Plastic Electronics, Exhibition Rd, London, SW7 2AZ, UK

○ Laboratoire de Chimie des Polymères Organiques – LCPO, UMR5629 Université de Bordeaux, Allée Geoffroy Saint Hilaire, Bâtiment B8 CS50023, 33615 Pessac Cedex, France

ABSTRACT: The optoelectronic landscape of conjugated polymers is intimately related to their molecular arrangement and packing, with minute changes in local order, such as chain conformation and torsional backbone order/disorder, frequently having a substantial effect on macroscopic properties. While many of these local features can be manipulated via chemical design, the synthesis of a series of compounds is often required to elucidate correlations between chemical structure and macromolecular ordering. Here, we show that blending semiconducting polymers with insulating commodity plastics enables controlled manipulation of the semiconductor backbone planarity. The key is to create a polarity difference between the semiconductor backbone and its side chains, while matching the polarity of the side chains and the additive. We demonstrate the applicability of this approach through judicious comparison of regioregular poly(3-hexylthiophene) (P3HT) with two of its more polar derivatives, namely the diblock copolymer poly(3-hexylthiophene)-block-poly(ethylene oxide) (P3HT-b-PEO) and the graft polymer poly[3-but(ethylene oxide)thiophene] (P3BEOT), as well as their blends with poly(ethylene oxide) (PEO). Proximity between polar side chains and a similarly polar additive reduces steric hindrance between individual chain segments by essentially 'expelling' the side chains away from the semiconducting backbones. This process, which has been shown to be facilitated via exposure to polar environments

such as humid air/water vapor, facilitates backbone realignment towards specific chain arrangements and, in particular, planar backbone configurations.

INTRODUCTION

In functional polymers, such as semiconducting plastics, chemical substitution with side chains is nowadays a frequently used strategy to manipulate and control the local macromolecular arrangement and packing, including torsional backbone order/disorder and lamellar- and π-stacking (see **Figure 1**).[1–4] This can affect — often strongly — contingent optoelectronic properties, such as charge-carrier transport[5–7] or absorption/emission features.[8–10] Originally, alkyl side chains were introduced to aid solubility and, generally, processability;[11] while more recently polar side chains, such as those based on oligo(ethylene oxide) groups, have attracted interest as they render the base material more compatible with so-called 'green' solvents.[12,13] Moreover, polymer semiconductors, substituted with polar side chains, are interesting for bioelectronic applications, for instance, where mixed electron/ion conduction is required (e.g., in electrochemical transistors used for biomimetic signal transduction, ion pumps, bioactive sensing elements), or where high biocompatibility is needed, including bio-integrated electronics and wearable devices.[14–19] However, side chains can inhibit backbone packing and aggregation, and often introduce undesired torsional backbone disorder. Hence, alternative approaches to control structural (and other) features of polymer semiconductors have been investigated, including blending with a second component, such as a commodity plastic.[20–24] This has been shown to provide an elegant pathway to expand the functionality of the semiconductor, perhaps best exemplified by blends of prototypical poly(3-hexyl thiophene) (P3HT) with bulk insulating plastics such as poly(ethylene oxide) (PEO) that can be manipulated to display drastically different absorption behavior compared to the neat semiconductor. This difference was tentatively attributed to a change in the torsional backbone order of P3HT.[20]

Here, we aim at combining these two approaches — chemical modification and blending — to control the molecular order of the active material and, thus, functionality. For this, we use model systems with the same conjugated backbone based on polythiophene chains — the P3HT homopolymer, the diblock copolymer poly(3-hexylthiophene)-block-poly(ethylene oxide) (P3HT-*b*-PEO),[25] and the graft polymer poly[3-but(ethylene oxide)thiophene] (P3BEOT; for chemical structures see Figure 1b,c insets) — and their blends with PEO. These judicious combinations of chemical structures and functionalities enables us to explore if blends can be designed from the outset such that the active material's

chain conformation and packing can be controlled by exploiting the different polarity-dependent compatibilities between certain moieties of the blend components. Indeed, the question we strive to answer is whether desirable macromolecular arrangements of polymeric semiconductors can be targeted by careful consideration of specific interactions between the semiconductor and the polymer 'additive'. Utilizing the sensitivity of the optical properties of polythiophenes and their derivatives to backbone configuration[26,27] thereby allows their local microstructure to be probed with a high degree of insight, providing a platform for future materials selection and processing criteria.

RESULTS AND DISUCSSION

We begin our discussion with the linear absorption and photoluminescence (PL) spectra of thin films of the three neat polymers: P3HT (molecular weight M_w = 100 kg mol^{-1}, dispersity Đ = 1.5, regioregularity 99%+) , P3HT$_{51}$-*b*-PEO$_{13}$ (M_w = 9.1 kg mol^{-1}), and P3BEOT (M_w = 23 kg mol^{-1}, Đ = 1.4, regioregularity 85%+) (Figure 1b,c; films wirebar coated in air from CHCl$_3$ solution with 10 mg ml^{-1} total polymer content). Immediately apparent from Figure 1b is that the PEO-block in P3HT-b-PEO has only a small effect on the characteristic optical features of the P3HT moiety. The 0-0/0-1 vibronic peak ratios both in absorption and emission, which are widely used sensitive indicators of the balance between intra- and inter-chain coupling,[26,28–31] are essentially identical for P3HT and P3HT-b-PEO. This is attributed to the P3HT segments in the block copolymer microphase separating from the PEO segments,[32–35] leaving the former virtually unaffected by the latter and, thus, keeping the typical characteristics of P3HT. In stark contrast, the P3BEOT graft copolymer displays significant spectral differences to the homopolymer, with only weak vibronic peaks observed in absorption at 560 and 610 nm. The absorption maximum is found at 450 nm. This blue shift relative to the P3HT homopolymer implies that P3BEOT comprises a larger fraction of non-aggregated, likely more torsionally disordered chain segments, similar to regiorandom P3HT (see Figure S1).[36] Support for this view is provided by the PL spectra of the graft copolymers, recorded at room temperature and 10 K, where we also observe a clear blue shift in spectral maxima, from 745 nm for the P3HT homopolymer to 595 nm for P3BEOT, accompanied by a clear loss of vibronic structure. Also noteworthy is the substantial overlap between absorption and emission spectra in P3BEOT, further reinforcing the picture that there is a significantly smaller fraction of torsionally ordered aggregates (with a smaller band gap) to which excitons can migrate prior to emission.[37]

2

When blending the three polymers with high molecular weight PEO (viscosity averaged molecular weight $M_v = 900$ kg mol^{-1}), following the procedures reported in Refs. 20 and 38, we find that adding PEO to the P3HT homopolymer leads to a substantially enhanced 0-0/0-1 peak ratio in both absorption and emission, entirely consistent with earlier observations[20] and characteristic of a transition from inter- to intra-molecular coupling[26,29,31] - similar changes in neat P3HT were previously attributed to polar solvent induced planarization in solution prior to aggregation.[39,40] In contrast, blending the block

copolymer P3HT-b-PEO with PEO has a negligible effect on the optical response of this P3HT copolymer. We again assign this observation to the tendency of block copolymers to microphase separate.[32–35] In a blend, the PEO blocks and PEO 'additive' can be expected to form relatively phase-pure microdomains, while the P3HT segments assemble in semiconductor-rich regions. This would drastically limit interactions of the PEO 'additive' and/or PEO blocks with semiconducting chain segments, in agreement with our findings.
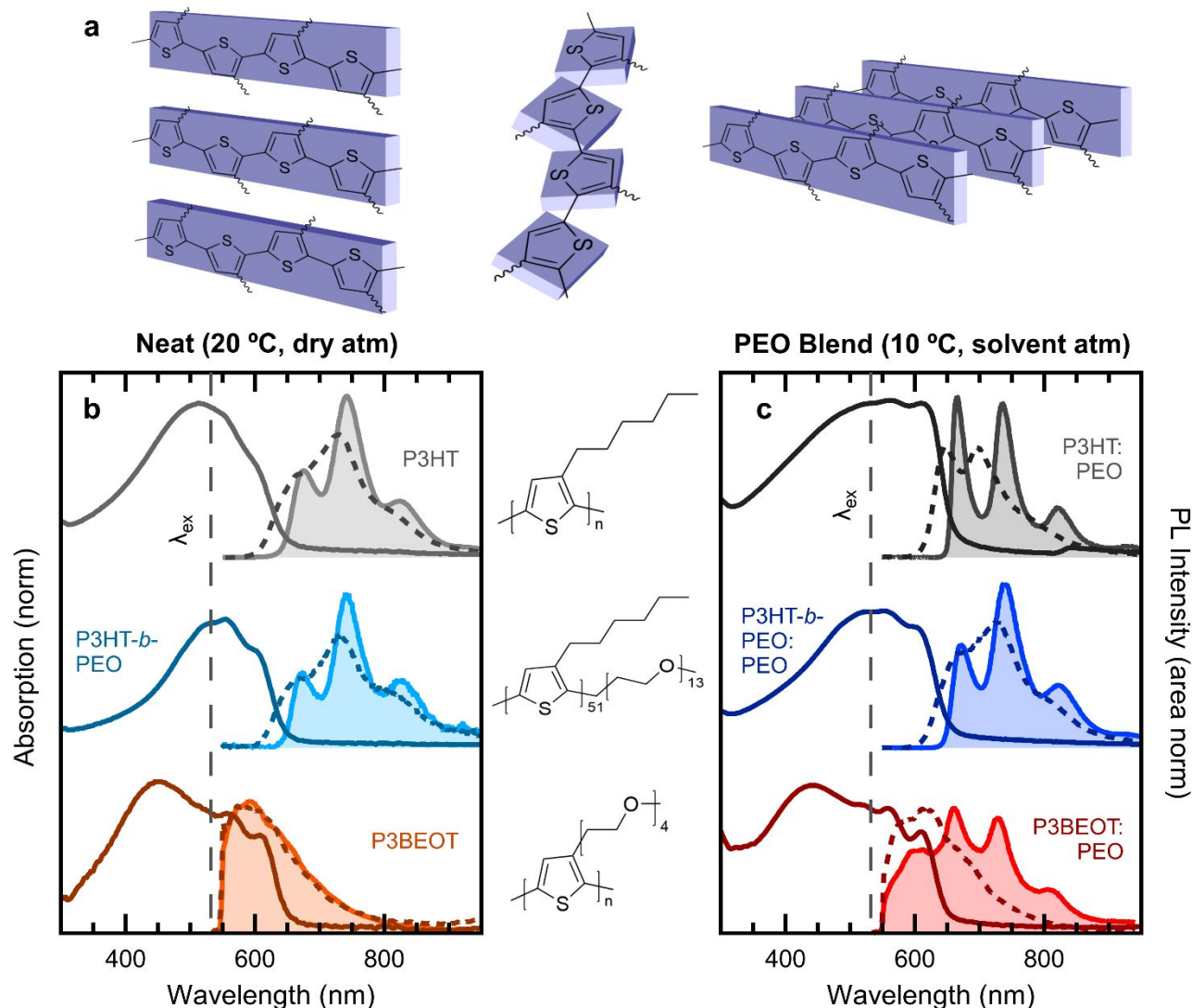

Figure 1. Schematic (a) showing three distinct types of local conjugated backbone order: lamellae (100) stacking (left), torsional disorder (center) and π-π (010) stacking (right). Normalized absorption and photoluminescence (PL) spectra of neat P3HT, P3HT-b-PEO and P3BEOT cast from solution at 20 °C (b), and 1:1 (weight%) blends with PEO (c), cast at 10 °C and dried within a solvent rich atmosphere. Absorption was determined at room temperature (solid line), and PL at RT (dashed) and 10 K (filled).

An entirely different scenario is observed for the P3BEOT:PEO blend. For this system, we find the most significant change in optical behavior upon blending — especially in PL. Unlike the spectrum of the neat graft copolymer, the blend exhibits clear vibronic structure at 10 K, although the emission spectrum characteristic of

non-aggregated polythiophene segments is still dominant (subtracting this disordered component reveals a clear similarity with P3HT:PEO, albeit with a lower 0-0/0-1 peak ratio – see Figure S2). Furthermore, comparison of total luminescence spectra for P3BEOT and P3BEOT:PEO reveal a substantially higher emission intensity from the

3

aggregated phase in the latter, relative to the non-aggregated phase (see Figure S3). Since this intensity variation is greater than the difference in absorption over the equivalent range of excitation wavelengths, this indicates a higher photoluminescent quantum yield in the blend, indicative of greater torsional order. Together, these changes imply that the high compatibility between the P3BEOT side chains and PEO via increased enthalpic interactions due to their mutual polarity leads to the inert component influencing the semiconducting backbone, affecting the latter's local assembly and hence its optoelectronic landscape. Notably, unlike the enhanced intra-molecular coupling in P3HT:PEO,[20] this process does not require a high molecular weight (M_w > entanglement threshold) semiconducting component.
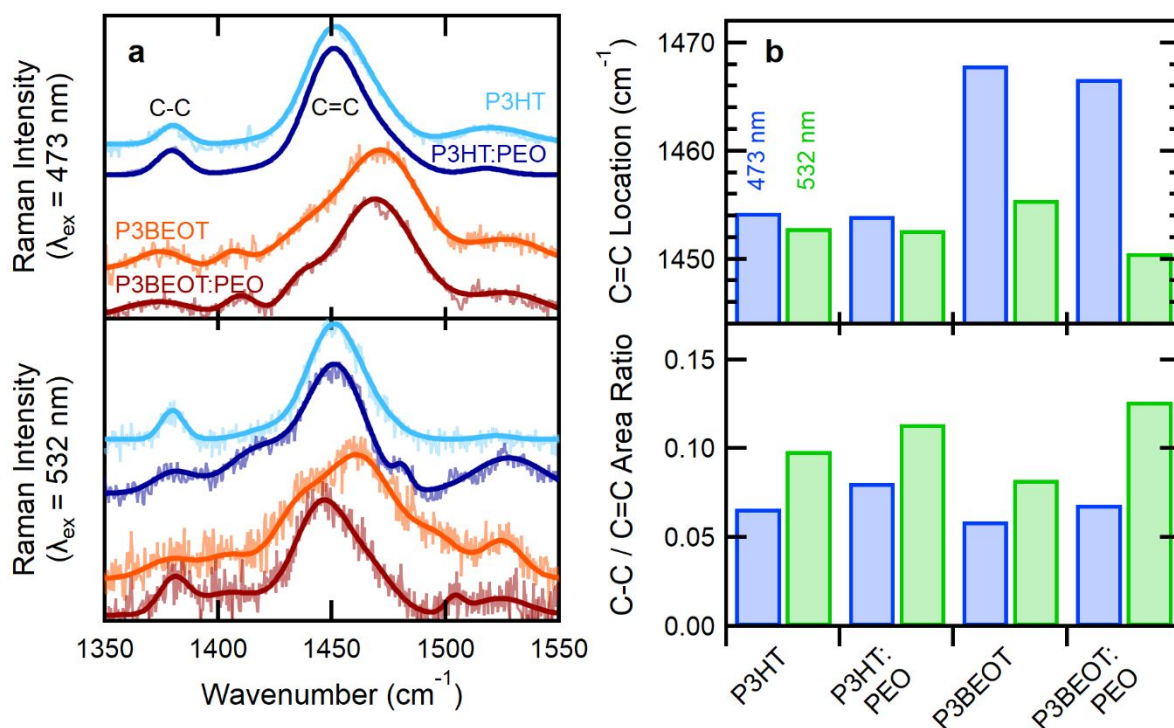

Figure 2. Normalized resonance Raman spectra (a) with λex = 473 (top) and 532 nm (bottom) of P3HT, P3HT:PEO, P3BEOT and P3BEOT:PEO, offset vertically for clarity. Original spectra are overlaid with fits (see Figure S4, S5). Extracted parameters (b) are the symmetric C=C stretching mode location (top) (an area weighted average of underlying peaks, higher values indicate increased torsional disorder) and C-C to C=C peak area ratio (bottom) (higher values indicate greater planarity).

Based on the aforementioned findings, the P3BEOT system was studied in greater detail, comparing it to P3HT and blends of both with PEO. Focus was placed on changes related to local ordering that could lead to the observed difference in the absorption and emission spectra between the neat P3BEOT and the P3BEOT:PEO binary blend, concentrating on torsional backbone order as analyzed by resonance Raman spectroscopy. This technique provides a sensitive probe of local molecular arrangement and conformation in polymer semiconductors, with selectivity achieved by exciting either non-aggregated or aggregated fractions at 473 and 532 nm, respectively. **Figure 2a** shows experimental resonance Raman spectra overlaid with peak fits corresponding to the C-C (~1380 cm⁻¹), symmetric C=C (~1450 to 1470 cm⁻¹) and asymmetric C=C (~1525 cm⁻¹) stretching modes (see Figure S4, S5 for fitting and residuals following excitation at 473 and 532 nm,

respectively).[41,42] Increased intensity of the C-C stretch relative to the dominant symmetric C=C mode, and a shift of the symmetric C=C band to lower frequencies, have previously been correlated with increased planarity between monomer units due to enhanced π-electron delocalization.[41,42] Therefore, the frequency of the symmetric C=C band and the C-C/C=C intensity ratio was followed to assess the torsional order of the polythiophene backbones in our systems, expecting C=C stretching vibrations for torsionally disordered chains to be around 1470 cm⁻¹ and those for planar chains around 1450 cm⁻¹. Turning attention to the neat materials (*i.e.*, P3BEOT and P3HT), when exciting their non-aggregated regions (λex = 473 nm), the symmetric C=C stretching band (an area-weighted average of two underlying peaks) appears at ~1465 cm⁻¹ and ~1454 cm⁻¹ for P3BEOT and P3HT, respectively (see Figure 2b, top panel; fits are presented in Figures S1 and S2). Probing more

4

aggregated domains (λ_{ex} = 532 nm), the symmetric C=C stretching mode was observed at ~1456 cm^{-1} for P3BEOT, while in P3HT this mode remains almost unchanged at ~1453 cm^{-1}. Taken together, these observations reinforce our interpretation of the absorption spectra (Figure 1b,c), specifically that the neat graft polymer is substantially more torsionally disordered than P3HT, particularly in the non-aggregated regions, with the aggregated regions comprising a certain fraction of segments of a similar backbone planarity to that found in P3HT. These regions are likely to be responsible for the weak vibronic structure shown in the UV-vis absorption spectrum of P3BEOT.

Moving on to the PEO binary blends, no significant effect on the symmetric C=C stretching peak location is found when adding PEO to P3HT regardless of λ_{ex}, *i.e.*, independent of whether aggregated or non-aggregated regions are probed. However, the C-C/C=C peak area ratio (see Figure 2b, bottom panel) increases slightly for the blend compared to neat P3HT, consistent with the addition of PEO slightly increasing P3HT backbone planarity. On the contrary, blending has a striking effect on P3BEOT. Introduction of PEO leads to a notable decrease in the symmetric C=C stretching mode frequency of ~5 cm^{-1} when probing aggregated regions (Figure 2b, top panel), resulting in a peak at ~1451 cm^{-1}. This frequency is slightly (~2 cm^{-1}) lower than found for neat P3HT and its blends with PEO, indicating that the addition of PEO to the graft polymer substantially increases the fraction of chain segments with increased backbone planarity, especially in aggregated regions, often beyond that achievable in neat or blended P3HT. This conclusion is supported by the C-C/C=C peak area ratio on probing aggregated regions (λ_{ex} = 532 nm); for P3BEOT:PEO, it is somewhat higher than for both P3HT and P3HT:PEO (Figure 2b, bottom panel).[41,42] In contrast, blending has a far less pronounced effect on the non-aggregated fraction (λ_{ex} = 473 nm), with the reduction in symmetric C=C location being comparatively negligible at ~1 cm^{-1}, and a smaller increase in C-C/C=C peak ratio found than when exciting the aggregated fraction.

Since the increased backbone planarity does not necessarily imply increased aggregation or even long range order (but will play a role in determining the balance between inter- and intra-chain coupling within aggregates),[26,31] grazing-incidence wide-angle X-ray scattering (GIWAXS) was performed to probe the crystalline ordering and orientation in the polymer systems.[43] Scattering patterns for P3BEOT and P3BEOT:PEO, and for comparison P3HT, P3HT:PEO and PEO, are shown in Figure S6, along with their scattered peak intensity along the out-of-plane (Q_z) direction. The neat P3BEOT graft polymer lacks pronounced lamellar scattering peaks, typical for systems with limited long-range order; despite this, weak features are evident at low

momentum transfer ($Q_z \leq 1$ Å^{-1}), indicating that a small proportion of chain segments display some propensity for translational order. Observations are very different for the blend, with P3BEOT:PEO showing a series of intense scattering peaks at low momentum transfer that cannot be attributed to PEO. Three scattering peaks can be seen at Q_z = 0.24, 0.48 and 0.72 Å^{-1}, with an interval of ~0.24 Å^{-1}, which we assign to the (100), (200) and (300) diffractions of the semiconductor. Accordingly, we infer a lamellar stacking distance of ~2.61 nm. This is larger than for the P3HT homopolymer, neat or blended with PEO, where the (100) diffraction is found at Q_z = 0.39 Å^{-1} (lamellae stacking distance ~1.61 nm), and can be attributed to the longer side chains of P3BEOT compared to P3HT. Indeed, this distance is close to those of poly(alkyl thiophene)s with similar side chain lengths to P3BEOT, such as poly(3-dodecyl thiophene) (P3DDT), with a Q_z peak at ~0.25 Å^{-1} (lamellae stacking distance ~2.51 nm)[44] — although the addition of PEO may also contribute to the observed effect. Our observations clearly show that in addition to affecting backbone planarity and smaller-scale aggregation, blending P3BEOT with PEO induces long-range packing that can be revealed by x-ray scattering – specifically, clear orientational order with P3BEOT lamellae stacking predominantly out-of-plane ((h00) peaks are only found along Q_z).

CONCLUSIONS

Blending with insulating polymers can be an efficient tool to manipulate the local, and to a certain extent long-range, arrangement of polymeric semiconductors. Microphase separation, as found in block copolymers (neat and in blends), has been shown to have little effect on local molecular ordering, whereas considerable structural changes can be induced in blends with graft polymers as the active component. For this to occur, it appears that two criteria must be satisfied: i) there must be a strong contrast in polarity between the semiconductor backbone and its side chains, and ii) there must be a strong affinity between the semiconductor side chains and the insulating polymer 'additive'. Such a scenario creates an enthalpic driving force that 'draws' the polar side chains away from the active material's backbone towards the second blend component, reducing the side chain disorder and, possibly, the steric hindrance that normally would lead to torsional disorder and reduced aggregation, especially in materials with relatively bulky side chains. These entropic interactions overcome the plasticizing effect of PEO, which lowers the fictive temperature (an experimentally accessible substitute for the glass transition temperature, T_g)[45] of P3BEOT in the blends by ~9 °C compared to the neat system (see Figure S7; with additional data for neat P3BEOT shown in Figure S8). In the absence of a polarity contrast, such a depression of the glass transition

temperature leads to more rapid segmental backbone relaxation, which in turn can be expected to lead to increased torsional backbone disorder. In contrast, in the case of high-polarity blends, the increased backbone mobility may assist in adopting a more planar backbone conformation, facilitating backbone re-arrangement.

The polarity contrast between backbone and side chains/additive can, of course, be manipulated in a rather straightforward fashion. For instance, herein insulating polymer 'additives' were selected that are structurally similar to PEO but have different Hansen Solubility Parameters and, therefore, have different interactions with the P3BEOT side chains – *i.e.,* a different polarity contrast (**Figure 3a** and SI).[46–49] Reassuringly, increasing the polarity of the 'additive polymer' leads to more pronounced vibronic structures in the PL of the blend when probing aggregated species (λ_{ex} = 580 nm; Figure 3b), and to a lower-frequency symmetric C=C band and correspondingly higher C-C/C=C peak ratio in resonant Raman spectroscopy (λ_{ex} = 532 nm; Figure 3c, spectra in Figure S9). These findings substantiate our interpretation that interactions between polar side chains and a similarly polar insulating 'additive' promote planarization of the semiconducting backbone by drawing away side chains and, thus, reducing steric hinderance. Polarity contrast is clearly critical. Examples of blends with strong affinity between the side chain and additive but with no polarity contrast between side chains/additive and the conjugated backbone of the main component, such as binary blends of poly[3-(2′-ethyl)-hexylthiophene] (P3EHT),[50] comprising a poly(thiophene) backbone with branched alkyl side chains, and ultra-low-density polyethylene (ULDPE), a highly branched version of polyethylene, show that blending has little effect on local order of the semiconductor (Figure S10).
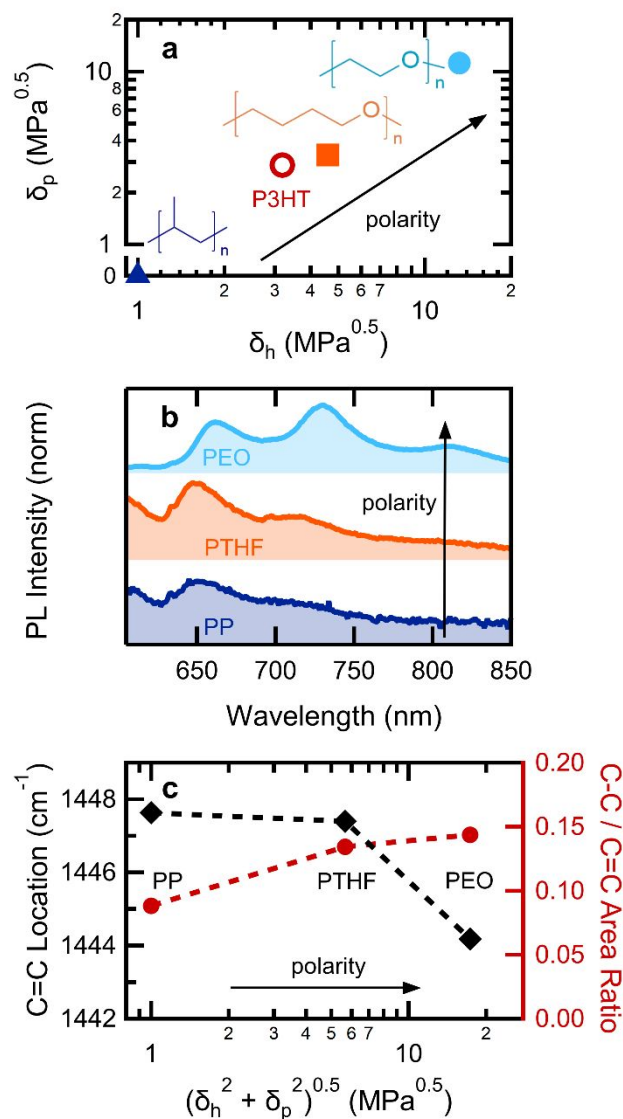

Figure 3. Insulating polymers (a) with different polar δ_p and hydrogen-bonding δ_h Hansen Solubility Parameters, were blended with P3BEOT. 10 K (b) PL of P3BEOT:PEO, P3BEOT:PTHF and P3BEOT:PP (λ_{ex} = 580 nm) shows an increase in vibronic structure with insulator polarity. Resonance Raman (c) symmetric C=C peak location decreases and C-C/C=C peak area ratio (λ_{ex} = 532 nm) increases with insulator polarity (distance from origin in (a)), indicating reduced torsional disorder (spectra, fits and residuals in Figure S9).

It should be noted that the local polarity environment can also be affected by small-molecular additives. This can be exemplified by experiments involving the controlled exposure of neat P3BEOT and its blend with PEO to water vapor. Water will increase the polarity contrast between backbone and side chains/PEO; it also will act as a plasticizer,[39,51] lowering the T_g of the neat P3BEOT and P3BEOT:PEO, as confirmed by fast differential scanning calorimetry measurements (DSC, Figure S11). Intuitively,

6

one would assume plasticization should increase the torsional backbone disorder of P3BEOT (as discussed above) leading to less electronic coupling between semiconducting chains and, hence, a weak vibronic structure in UV-vis absorption and PL spectra. However, after incorporating water into P3BEOT and P3BEOT:PEO blends *via* exposure to water vapor, both systems display a more pronounced vibronic structure both in absorption and PL (see Figure S12), from which we infer that also this treatment leads to higher torsional backbone order, with the effect being notably stronger for the blends.

The effect of small-molecular additives is, however, not necessarily stable. This is reflected by the structural evolution of P3BEOT and its blends with PEO directly after casting and drying — a process where humidity is trapped in the resulting thin films — and after aging over a period of four months in ambient conditions, as followed by resonance Raman spectroscopy. For the neat graft copolymer, when exciting aggregated regions (λ_{ex} = 532 nm), the frequency of its symmetric C=C stretching mode initially is, intriguingly, very low (~1447 cm^{-1}) and comparable to that of P3BEOT:PEO (~1444 cm^{-1}, Figure S13, fits shown in Figure S14). This implies that, initially, the neat graft copolymer comprises a high fraction of planar chain segments. However, this dominant mode shifts over time to higher frequencies until 'saturating' after four months at ~1456 cm^{-1}, accompanied by a noticeable reduction in C-C/C=C peak area ratio. In stark contrast, the polymer blend is markedly more stable over time with respect to structure. A change in peak frequency in the blend is observed over time, but one that is drastically smaller than that observed for the neat graft polymer, with aged samples featuring a symmetric C=C stretching mode at ~1450 cm^{-1} accompanied by a slight decrease in C-C/C=C peak ratio. This C=C stretching mode frequency is still slightly smaller than what is found for neat P3HT, while the C-C/C=C peak ratio is higher, which shows that in P3BEOT:PEO blends, the P3BEOT backbone segments remain more planar than in P3HT and P3HT:PEO binary blends, also when aged for four months (Figure S13b). We attribute the instability of the planarization effect of water/humidity in neat P3BEOT to the relatively rapid release of water from this system. In contrast, water molecules retained in the P3BEOT:PEO binary blends due to the hydrophilic PEO[52,53] stay trapped, contributing to the polarity contrast and assisting in planarizing the semiconductor backbone. This is supported by UV-vis and PL spectroscopy (see SI, Figure S12) and highlights the benefit of blending with polymeric matrices.

The moisture dependence of P3BEOT and its blends with PEO further emphasizes the strong correlation between local environment and backbone ordering (and consequently, optical response), and hence the wide applicability via selection of side chain polarity, polarity of blend component as well as small-molecular additives, such as water, that further affect the polarity contrast between backbone and environment. Our findings, thus, open a simple alternative pathway to structural control without the need to realize all functionality exclusively via (often complex) chemical design. This approach will be particularly important in fields where materials comprising bulky side chains are used – for instance, bioelectronics where more polar moieties are frequently added to the active material to increase biocompatibility, increase water-induced swelling and enhance ion flow. In these scenarios, blending should allow for control of local ordering and packing, while side chain substitution can be used to introduce other desired functionalities.

ASSOCIATED CONTENT

Supporting Information. Experimental methods, further discussion of GIWAXS, solubility and humidity, further analysis of absorption and PL spectra, site-selective PL and total luminescence spectra, additional Raman spectra and fitting, fast-DSC scans and analysis, GIWAXS measurements, humidity dependent absorption and PL spectra, synthetic methods, NMR spectra. Supporting Information is available free of charge via the Internet at http://pubs.acs.org.

AUTHOR INFORMATION

Corresponding Author

*Email: (M.D.) m.j.dyson@tue.nl

*Email: (S.H.) shayes@ucy.ac.cy

*Email: (N.S.) natalie.stingelin@mse.gatech.edu

Notes

The authors declare no competing financial interests.

ACKNOWLEDGMENT

7

Atlanta, Georgia, USA) and Prof. Iain McCulloch (Physical Sciences and Engineering Division, King Abdullah University of Science and Technology (KAUST), Saudi Arabia) for many helpful discussions.

REFERENCES

(1) Mei, J.; Bao, Z. Side Chain Engineering in Solution-Processable Conjugated Polymers. *Chem. Mater.* **2014**, *26*, 604–615.

(2) Himmelberger, S.; Duong, D. T.; Northrup, J. E.; Rivnay, J.; Koch, F. P. V; Beckingham, B. S.; Stingelin, N.; Segalman, R. A.; Mannsfeld, S. C. B.; Salleo, A. Role of Side-Chain Branching on Thin-Film Structure and Electronic Properties of Polythiophenes. *Adv. Funct. Mater.* **2015**, *25*, 2616–2624.

(3) Duan, C.; Willems, R. E. M.; van Franeker, J. J.; Bruijnaers, B. J.; Wienk, M. M.; Janssen, R. A. J. Effect of Side Chain Length on the Charge Transport, Morphology, and Photovoltaic Performance of Conjugated Polymers in Bulk Heterojunction Solar Cells. *J. Mater. Chem. A* **2016**, *4*, 1855–1866.

(4) Kim, J.-H.; Wood, S.; Park, J. B.; Wade, J.; Song, M.; Yoon, S. C.; Jung, I. H.; Kim, J.-S.; Hwang, D.-H. Optimization and Analysis of Conjugated Polymer Side Chains for High-Performance Organic Photovoltaic Cells. *Adv. Funct. Mater.* **2016**, *26*, 1517–1525.

(5) Kumar, A.; Baklar, M. A.; Scott, K.; Kreouzis, T.; Stingelin-Stutzmann, N. Efficient, Stable Bulk Charge Transport in Crystalline/Crystalline Semiconductor-Insulator Blends. *Adv. Mater.* **2009**, *21*, 4447–4451.

(6) Han, S.; Yu, X.; Shi, W.; Zhuang, X.; Yu, J. Solvent-Dependent Electrical Properties Improvement of Organic Field-Effect Transistor Based on Disordered Conjugated Polymer/Insulator Blends. *Org. Electron.* **2015**, *27*, 160–166.

(7) Ong, B. S.; Wu, Y.; Liu, P.; Gardner, S. High-Performance Semiconducting Polythiophenes for Organic Thin-Film Transistors. *J. Am. Chem. Soc.* **2004**, *126*, 3378–3379.

(8) Delongchamp, D. M.; Kline, R. J.; Fischer, D. A.; Richter, L. J.; Toney, M. F. Molecular Characterization of Organic Electronic Films. *Adv. Mater.* **2011**, *23*, 319–337.

(9) Botiz, I.; Astilean, S.; Stingelin, N. Altering the Emission Properties of Conjugated Polymers. *Polym. Int.* **2016**, *65*, 157–163.

(10) Raithel, D.; Simine, L.; Pickel, S.; Schötz, K.; Panzer, F.; Baderschneider, S.; Schiefer, D.; Lohwasser, R.; Köhler, J.; Thelakkat, M.; et al. Direct Observation of Backbone Planarization via Side-Chain Alignment in Single Bulky-Substituted Polythiophenes. *Proc. Natl. Acad. Sci.* **2018**, *115*, 2699–2704.

(11) Roncali, J. Conjugated Poly(Thiophenes): Synthesis , Functionalization , and Applications. *Chem. Rev.* **1992**, *92*, 711–738.

(12) Chen, X.; Zhang, Z.; Ding, Z.; Liu, J.; Wang, L. Diketopyrrolopyrrole-Based Conjugated Polymers Bearing Branched Oligo(Ethylene Glycol) Side Chains for Photovoltaic Devices. *Angew. Chemie - Int. Ed.* **2016**, *55*, 10376–10380.

(13) Lee, C.; Lee, H. R.; Choi, J.; Kim, Y.; Nguyen, T. L.; Lee, W.; Gautam, B.; Liu, X.; Zhang, K.; Huang, F.; et al. Efficient and Air-Stable Aqueous-Processed Organic Solar Cells and Transistors: Impact of Water Addition on Processability and Thin-Film Morphologies of Electroactive Materials. *Adv. Energy Mater.* **2018**, 1802674.

(14) Giovannitti, A.; Sbircea, D.-T.; Inal, S.; Nielsen, C. B.; Bandiello, E.; Hanifi, D. A.; Sessolo, M.; Malliaras, G. G.; McCulloch, I.; Rivnay, J. Controlling the Mode of Operation of Organic Transistors through Side-Chain Engineering. *Proc. Natl. Acad. Sci.* **2016**, *113*, 12017–12022.

(15) Pacheco-Moreno, C. M.; Schreck, M.; Scaccabarozzi, A. D.; Bourgun, P.; Wantz, G.; Stevens, M. M.; Dautel, O. J.; Stingelin, N.; Gerhardt, I. C.; Alberto, D.; et al. The Importance of Materials Design to Make Ions Flow : Toward Novel Materials Platforms for Bioelectronics Applications. *Adv. Mater.* **2017**, *29*, 1604446.

(16) Rivnay, J.; Owens, R. M. R. M.; Malliaras, G. G. The Rise of Organic Bioelectronics. *Chem. Mater.* **2014**, *26*, 679–685.

(17) Simon, D. T.; Gabrielsson, E. O.; Tybrandt, K.; Berggren, M. Organic Bioelectronics: Bridging the Signaling Gap between Biology and Technology. *Chem. Rev.* **2016**, *116*, 13009–13041.

(18) Nielsen, C. B.; Giovannitti, A.; Sbircea, D.; Bandiello, E.; Niazi, M. R.; Hanifi, D. A.; Sessolo, M.; Amassian, A.; Malliaras, G. G.; Rivnay, J.; et al. Molecular Design of Semiconducting Polymers for High- Performance Organic Electrochemical Transistors. *J. Am. Chem. Soc.* **2016**, *138*, 10252–10259.

(19) Giovannitti, A.; Nielsen, C. B.; Sbircea, D. T.; Inal, S.; Donahue, M.; Niazi, M. R.; Hanifi, D. A.; Amassian, A.; Malliaras, G. G.; Rivnay, J.; et al. N-Type Organic Electrochemical Transistors with Stability in Water. *Nat. Commun.* **2016**, *7*, 13066.

(20) Hellmann, C.; Paquin, F.; Treat, N. D.; Bruno, A.; Reynolds, L. X.; Haque, S. A.; Stavrinou, P. N.; Silva, C.; Stingelin, N. Controlling the Interaction of Light with Polymer Semiconductors. *Adv. Mater.* **2013**, *25*, 4906–4911.

(21) Scaccabarozzi, A. D.; Stingelin, N. Semiconducting:Insulating Polymer Blends for Optoelectronic Applications—a Review of Recent Advances. *J. Mater. Chem. A* **2014**, *2*, 10818–10824.

(22) Jahnke, A. A.; Yu, L.; Coombs, N.; Scaccabarozzi, A. D.; Tilley, A. J.; Dicarmine, P. M.; Amassian, A.; Stingelin, N.; Seferos, D. S. Polytellurophenes Provide Imaging Contrast towards Unravelling the Structure-Property-Function Relationships in Semiconductor: Insulator Polymer Blends. *J. Mater. Chem. C* **2015**, *3*, 3767–3773.

(23) Strobel, N.; Eckstein, R.; Lehr, J.; Lemmer, U.; Hernandez-sosa, G. Semiconductor:Insulator Blends for Speed Enhancement in Organic Photodiodes. *Adv. Electron. Mater.* **2017**, *4*, 1700345.

(24) Abbaszadeh, D.; Kunz, A.; Wetzelaer, G. A. H. H.; Michels, J. J.; Crăciun, N. I.; Koynov, K.; Lieberwirth, I.; Blom, P. W. M. M. Elimination of Charge Carrier Trapping in Diluted Semiconductors. *Nat. Mater.* **2016**, *15*, 628–633.

(25) Erothu, H.; Sohdi, A. A.; Kumar, A. C.; Sutherland, A. J.; Dagron-Lartigau, C.; Allal, A.; Hiorns, R. C.; Topham, P. D. Facile Synthesis of Poly(3-Hexylthiophene)-Block-Poly(Ethylene Oxide) Copolymers via Steglich Esterification. *Polym. Chem.* **2013**, *4*, 3652–3655.

(26) Niles, E. T.; Roehling, J. D.; Yamagata, H.; Wise, A. J.; Spano, F. C.; Moulé, A. J.; Grey, J. K. J-Aggregate Behavior in Poly-3-Hexylthiophene Nanofibers. *J. Phys. Chem. Lett.* **2012**, *3*, 259–263.

(27) Grégoire, P.; Vella, E.; Dyson, M.; Bazán, C. M.; Leonelli, R.; Stingelin, N.; Stavrinou, P. N.; Bittner, E. R.; Silva, C.; Gregorie, P.; et al. Excitonic Coupling Dominates the Homogeneous Photoluminescence Excitation Linewidth in Semicrystalline Polymeric Semiconductors. *Phys. Rev. B* **2017**, *95*, 180201(R).

(28) Clark, J.; Silva, C.; Friend, R.; Spano, F. C. Role of Intermolecular Coupling in the Photophysics of Disordered Organic Semiconductors: Aggregate Emission in Regioregular Polythiophene. *Phys. Rev. Lett.* **2007**, *98*,

8

206406.

(29) Paquin, F.; Yamagata, H.; Hestand, N. J.; Sakowicz, M.; Bérubé, N.; Côté, M.; Reynolds, L. X.; Haque, S. A.; Stingelin, N.; Spano, F. C.; et al. Two-Dimensional Spatial Coherence of Excitons in Semicrystalline Polymeric Semiconductors: Effect of Molecular Weight. *Phys. Rev. B* **2013**, *88*, 155202.

(30) Yamagata, H.; Spano, F. C. Interplay between Intrachain and Interchain Interactions in Semiconducting Polymer Assemblies: The HJ-Aggregate Model. *J. Chem. Phys.* **2012**, *136*, 184901.

(31) Spano, F. C.; Silva, C. H- and J-Aggregate Behavior in Polymeric Semiconductors. *Annu. Rev. Phys. Chem.* **2014**, *65*, 477–500.

(32) Patel, S. N.; Javier, A. E.; Beers, K. M.; Pople, J. A.; Ho, V.; Segalman, R. A.; Balsara, N. P. Morphology and Thermodynamic Properties of a Copolymer with an Electronically Conducting Block: Poly(3-Ethylhexylthiophene)-Block-Poly(Ethylene Oxide). *Nano Lett.* **2012**, *12*, 4901–4906.

(33) Park, S.; Kang, S.; Fryd, M.; Saven, J. G.; Park, S. Highly Tunable Photoluminescent Properties of Amphiphilic Conjugated Block-Copolymers Highly Tunable Photoluminescent Properties of Amphiphilic Conjugated Block- Copolymers. *J. Am. Chem. Soc.* **2010**, *132*, 9931–9933.

(34) Erothu, H.; Kolomanska, J.; Johnston, P.; Schumann, S.; Deribew, D.; Toolan, D. T. W.; Gregori, A.; Dagron-Lartigau, C.; Portale, G.; Bras, W.; et al. Synthesis, Thermal Processing, and Thin Film Morphology of Poly(3-Hexylthiophene)-Poly(Styrenesulfonate) Block Copolymers. *Macromolecules* **2015**, *48*, 2107–2117.

(35) Topham, P. D.; Parnell, A. J.; Hiorns, R. C. Block Copolymer Strategies for Solar Cell Technology. *J. Polym. Sci. Part B Polym. Phys.* **2011**, *49*, 1131–1156.

(36) Korovyanko, O.; Österbacka, R.; Jiang, X.; Vardeny, Z.; Janssen, R. Photoexcitation Dynamics in Regioregular and Regiorandom Polythiophene Films. *Phys. Rev. B* **2001**, *64*, 235122.

(37) Hoffmann, S. T.; Bässler, H.; Koenen, J. M.; Forster, M.; Scherf, U.; Scheler, E.; Strohriegl, P.; Köhler, A. Spectral Diffusion in Poly(Para-Phenylene)-Type Polymers with Different Energetic Disorder. *Phys. Rev. B* **2010**, *81*, 115103.

(38) Zhao, K.; Yu, X.; Li, R.; Amassian, A.; Han, Y. Solvent-Dependent Self-Assembly and Ordering in Slow-Drying Drop-Cast Conjugated Polymer Films. *J. Mater. Chem. C* **2015**, *3*, 9842–9848.

(39) Scharsich, C.; Lohwasser, R. H.; Sommer, M.; Asawapirom, U.; Scherf, U.; Thelakkat, M.; Neher, D.; Köhler, A. Control of Aggregate Formation in Poly(3-Hexylthiophene) by Solvent, Molecular Weight, and Synthetic Method. *J. Polym. Sci. Part B Polym. Phys.* **2012**, *50*, 442–453.

(40) Panzer, F.; Bässler, H.; Köhler, A. Temperature Induced Order-Disorder Transition in Solutions of Conjugated Polymers Probed by Optical Spectroscopy. *J. Phys. Chem. Lett.* **2017**, *8*, 114–125.

(41) Gao, Y.; Grey, J. K. Resonance Chemical Imaging of Polythiophene/Fullerene Photovoltaic Thin Films: Mapping Morphology-Dependent Aggregated and Unaggregated C=C Species. *J. Am. Chem. Soc.* **2009**, *131*, 9654–9662.

(42) Tsoi, W. C.; James, D. T.; Kim, J. S.; Nicholson, P. G.; Murphy, C. E.; Bradley, D. D. C.; Nelson, J.; Kim, J. S. The Nature of In-Plane Skeleton Raman Modes of P3HT and Their Correlation to the Degree of Molecular Order in P3HT:PCBM Blend Thin Films. *J. Am. Chem. Soc.* **2011**, *133*, 9834–9843.

(43) Rivnay, J.; Mannsfeld, S. C. B.; Miller, C. E.; Salleo, A.; Toney, M. F. Quantitative Determination of Organic Semiconductor Microstructure from the Molecular to Device Scale. *Chem. Rev.* **2012**, *112*, 5488–5519.

(44) Sauvé, G.; Javier, A. E.; Zhang, R.; Liu, J.; Sydlik, S. A.; Kowalewski, T.; McCullough, R. D. Well-Defined, High Molecular Weight Poly(3-Alkylthiophene)s in Thin-Film Transistors: Side Chain Invariance in Field-Effect Mobility. *J. Mater. Chem.* **2010**, *20*, 3195–3201.

(45) Badrinarayanan, P.; Zheng, W.; Li, Q.; Simon, S. L. The Glass Transition Temperature versus the Fictive Temperature. *J. Non. Cryst. Solids* **2007**, *353*, 2603–2612.

(46) Barton, A. F. M. Solubility Parameters. *Chem. Rev.* **1975**, *75*, 731–753.

(47) Hansen, C. M. *Hansen Solubility Parameters: A User's Handbook*, 2nd ed.; CRC Press: Boca Raton, FL, USA, 2007.

(48) Duong, D. T.; Walker, B.; Lin, J.; Kim, C.; Love, J.; Purushothaman, B.; Anthony, J. E.; Nguyen, T. Q. Molecular Solubility and Hansen Solubility Parameters for the Analysis of Phase Separation in Bulk Heterojunctions. *J. Polym. Sci. Part B Polym. Phys.* **2012**, *50*, 1405–1413.

(49) Huang, J. C.; Deanin, R. D.; Jan-Chan Huang, R. D. D.; Huang, J. C.; Deanin, R. D. Multicomponent Solubility Parameters of Poly(Vinyl Chloride) and Poly(Tetramethylene Glycol). *Fluid Phase Equilib.* **2005**, *227*, 125–133.

(50) Boudouris, B. W.; Ho, V.; Jimison, L. H.; Toney, M. F.; Salleo, A.; Segalman, R. A. Real-Time Observation of Poly(3-Alkylthiophene) Crystallization and Correlation with Transient Optoelectronic Properties. *Macromolecules* **2011**, *44*, 6653–6658.

(51) Levine, H.; Slade, L. Water as a Plasticizer: Physico-Chemical Aspects of Low-Moisture Polymeric Systems. In *Water Science Reviews 3*; 2016; pp 79–185.

(52) Kjellander, R.; Florin, E. Water Structure and Changes in Thermal Stability of the System Poly (Ethylene Oxide)–water. *J. Chem. Soc. Faraday Trans. 1* **1981**, *77*, 2053–2077.

(53) Carlsson, M.; Hallenf, D.; Linse, P.; Hallen, D.; Linse, P. Mixing Enthalpy and Phase Separation in a Poly(Propylene Oxide) -Water System. *J. Chem. Soc. Faraday Trans.* **1995**, *91*, 2081–2085.

1
2
3
4
5
6
7
8
9
10
11
12
13
14
15
16
17
18
19
20
21
22
23
24
25
26
27
28
29
30
31
32
33
34
35
36
37
38
39
40
41
42
43
44
45
46
47
48
49
50
51
52
53
54
55
56
57
58
59
60

9

1
2
3
4
5
6
7
8
9
10
11
12
13
14
15
16
17
18
19
20
21
22
23
24
25
26
27
28
29
30
31
32
33
34
35
36
37
38
39
40
41
42
43
44
45
46
47
48
49
50
51
52
53
54
55
56
57
58
59
60